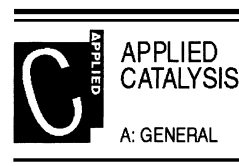




ELSEVIER

Applied Catalysis A: General 181 (1999) 289–303



m-Xylene reactions over zeolites with unidimensional pore systems

Christopher W. Jones^a, Stacey I. Zones^b, Mark E. Davis^{a,*}

^aCalifornia Institute of Technology, Chemical Engineering, Pasadena, CA 91125, USA

^bChevron Research and Technology Company, Richmond, CA 94802, USA

Received 19 May 1998; received in revised form 12 September 1998; accepted 5 November 1998

Abstract

Reactions of *m*-xylene are performed over a series of unidimensional, high-silica zeolites. It is determined that zeolites with a unidimensional pore structure have a unique reaction selectivity when compared to multidimensional zeolites of the same pore size. Unlike multidimensional zeolites with 12 member ring (MR) pores that give a *para/ortho* (*p/o*) selectivity of >1, zeolites with unidimensional pores bounded by 14 MRs or large 12 MRs give a *p/o* <1 due to the influence of a bimolecular isomerization mechanism between a xylene and trimethylbenzene. The unidimensional, parallel pore zeolites (UTD-1, SSZ-31, CIT-5, SSZ-24, ZSM-12, ZSM-48) gave products with the lowest *p/o* ratio for the given pore size. Multidimensional zeolites and unidimensional zeolites with internal cavities larger than the pore openings all gave higher *p/o* selectivities. It is shown that at lower flow rates, where external diffusion becomes important, *p/o* selectivity can be lowered due to an increased amount of bimolecular isomerization occurring at or near the catalyst external surface. While the selectivity of the reactions of *m*-xylene give useful information for characterizing zeolite structures, it is imperative that all zeolites be compared at the same flow rate and that the flow rate be sufficiently high to negate significant external diffusion effects on reaction selectivity. Under the proper conditions, the reactions of *m*-xylene can give information enabling the characterization of medium, large and extra-large pore zeolites. © 1999 Elsevier Science B.V. All rights reserved.

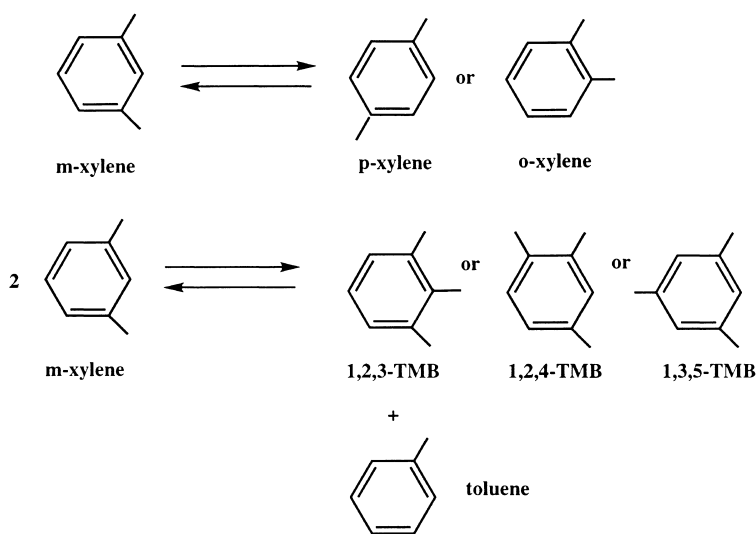
Keywords: Test reaction; *m*-Xylene; External surface reaction; Zeolite

1. Introduction

Catalytic test reactions are valuable tools for the characterization of molecular sieve structures in that they provide crucial insights into the pore architecture and catalytic activity of new molecular sieve materials whose structures are unknown and/or poorly characterized. When catalytic test results are combined with modern sorption and crystallographic techniques, relatively rapid determination of zeolite structures is

possible [1]. For example, Jacobs and coworkers [2] and Corma et al. [3] proposed in 1994 that the then unknown structure of the zeolite MCM-22 (MWW) contained both 10 MR and 12 MR channels based on sorption and catalytic data. In addition, Corma et al. [3], using catalytic data from two test reactions, proposed that the 10 MR and 12 MR channels gave free spaces of larger diameter within the zeolite pore system. That year, the crystal structure was determined by researchers at Mobil using a combination of high resolution electron micrographs and synchrotron X-ray powder diffraction patterns [4]. The published zeolite structure did indeed have both 12 MR

*Corresponding author. Tel.: +1-626-3954251; fax: +1-626-5688743; e-mail: mdavis@cheme.caltech.edu



Scheme 1.

and 10 MR with large cages of $7.1 \text{ \AA} \times 18.2 \text{ \AA}$, as proposed by Corma et al. [3].

m-Xylene isomerization and disproportionation have been used by a number of groups for the characterization of acidic zeolites, e.g. [1,3,5].

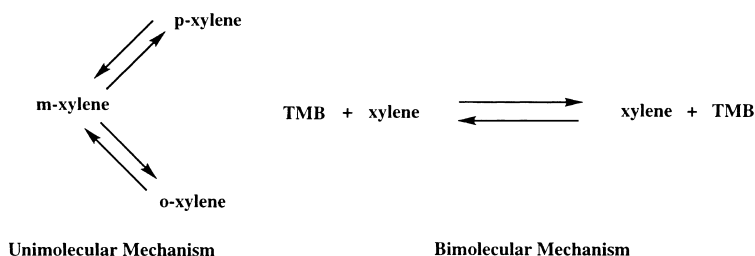
m-Xylene isomerizes to the *para* and *ortho* isomers and can disproportionate into trimethylbenzenes (TMBs) and toluene as illustrated in Scheme 1.

Four key parameters can be determined from the catalytic data of *m*-xylene reactions over acid catalysts. The *para/ortho* (*p/o*) ratio of the products gives insight into the catalyst pore size, with larger values corresponding to smaller pores and vice versa. The distribution of trimethylbenzenes can give useful information about the pore structure of zeolites. In zeolites with 12 MR, Martens et al. [5] showed that zeolites with adjacent cages or lobes favor the formation of the bulky 1,3,5-trimethylbenzene isomer while zeolites with straight channels and side pockets at regular distances, such as mordenite (MOR), are favorable for the formation of the 1,2,3-trimethylbenzene isomer. The ratio of the rates of isomerization to disproportionation (*ild*), like *p/o*, is useful for elucidating the pore or cage size. Since disproportionation necessarily requires a bimolecular reaction, larger pore systems that can accommodate the required transition state give more disproportionation. Although it is expected that the *ild* ratio does provide

information that can relate to the zeolite pore system, it has been experimentally found to be not that useful when compared to the *p/o* ratio and the distribution of TMB isomers [1,6]. Finally, the *m*-xylene reactions can provide a way of ascertaining rates of deactivation via carbon depositing mechanisms [6].

It has been demonstrated that isomerization can occur over aluminosilicates through both a bimolecular and unimolecular mechanism as shown in Scheme 2 [7,8].

Throughout the 1980s, researchers invoked only the unimolecular, 1,2-methyl shift mechanism of isomerization when analyzing *m*-xylene transformations over zeolites. Recently, Corma et al. [9,10] and Guisnet et al. [11] have reported that the bimolecular isomerization mechanism is important in zeolites with larger pores. Corma and Sastre [10] showed through isotopic labeling studies that the bimolecular pathway contributes to the reaction products in the 12 MR zeolites HY and H-mordenite. In contrast, isomerization over H-beta, another 12 MR zeolite, does not occur via the bimolecular pathway at low levels of conversion. Guisnet and coworkers [11] developed an interesting scheme to estimate the contribution of the bimolecular pathway to isomerization by determining the *p/o* selectivity of both isomerization mechanisms and calculating the contribution of each mechanism with a simple relation. They found that for HY, roughly



Scheme 2.

20% of the isomerization occurs via the bimolecular mechanism, which agrees with the work of Corma and Sastre [10]. With zeolites where this bimolecular isomerization mechanism operates, *p/o* ratios below the thermodynamic ratio of approximately 1 are possible. This is due to the distinctly different reaction selectivity of the bimolecular isomerization reaction. It has been demonstrated that the bimolecular reaction over HY has *p/o* value of 0.275 [11]. This is markedly different from the value of 1.18 for the monomolecular mechanism.

It is expected that in large and extra-large pore materials, where it is likely that the bimolecular mechanism is quite important, it may be possible to obtain *p/o* values below 1. Indeed, Guisnet and coworkers [12] have shown that *m*-xylene conversion over acidic MCM-41 mesoporous aluminosilicates is dominated by the bimolecular mechanism. While two operating isomerization mechanisms make for more complex kinetic analysis [13], we show that the *p/o* selectivity of the reaction can be used as a simple tool to characterize zeolite pore architecture. Here we describe the reactions of *m*-xylene over a series of unidimensional medium pore (10 MR), large pore (12 MR) and extra-large pore materials (12+MR). This work extends the previous study of *m*-xylene conversions over materials that have both 10 and 12 MR pores [6].

2. Experimental

2.1. Materials

A series of high-silica, unidimensional acidic molecular sieves (ZSM-48, ZSM-12, SSZ-24, SSZ-31,

SSZ-35, SSZ-42, SSZ-44, CIT-5, and UTD-1) were tested as catalysts for the transformation of *m*-xylene. In addition, several other zeolites were used for comparative purposes (SSZ-33, MOR, L, Beta, USY, OFF, ZSM-5).

CIT-5 was synthesized using a method described elsewhere [14] in the gallosilicate form. The material was calcined at 725°C to remove the structure-directing agent (SDA), then ion-exchanged three times with a 1.0 N NH₄NO₃ solution for 24 h at ~80°C.

SSZ-33 was prepared via a procedure described previously [15]. The boron form was transformed to the acidic aluminum form by a method already described [16,17].

Offretite was synthesized using tetramethylammonium hydroxide as an SDA. The as-synthesized material was calcined at 550°C and ion-exchanged three times with 1.0 N NH₄NO₃ solution for 24 h at ~80°C.

All other catalysts were provided by the Chevron Research and Technology Company. USY (PQ CBV 760), MOR (Tosoh HSZ-640HOA), ZSM-12, Beta, and ZSM-5 were provided in the proton form. ZSM-48, SSZ-42 and SSZ-44 were obtained in ammonium form. Al-UTD-1 was prepared according to [18]. SSZ-31 and SSZ-35 were obtained in Na-form and L (Tosoh, TSZ-500KOA) was obtained in K-form. These catalysts were subsequently ion-exchanged three times with a 1.0 N NH₄NO₃ solution for 24 h at ~80°C. All ammonium-exchanged samples were calcined to 550°C to generate the proton form prior to catalysis.

All samples were pressed into binder-free pellets, crushed and size sorted. Particles of size -35/+70 (US Standard mesh) were used for catalytic testing. The pore architecture of each material is described in Table 1.

Table 1
Catalyst characteristics

Sample	Si/Al ^a	Si/Al framework ^b	Crystal size ^c	Pore structure	Dimensionality
ZSM-48	55.0	ND	2–4 μm	10 MR, 5.6 Å×5.3 Å	1D
ZSM-12	42.0	44.0	Submicron	Constrained 12 MR, 5.9 Å×5.5 Å	1D
SSZ-24	39.0	40.5	Submicron	12 MR, 7.3 Å	1D
SSZ-31	39.5	42.0	Submicron	Elliptical 12 MR, 8.6 Å×5.7 Å	1D
SSZ-35	35.0	36.0	Sub-2 μm	10 MR, stacked cages, 5.65 Å	1D
SSZ-42	18.0	18.5	1 μm	Undulating 12 MR, 6.7 Å	1D
SSZ-44	29.0	30.0	3–7 μm	10 MR, stacked cages, 5.75 Å	1D
CIT-5	94.5 ^d	ND	Sub-3 μm	Constrained 14 MR, 7.3 Å	1D
UTD-1	34.5	38.5	Submicron	14 MR, 7.5 Å×10 Å	1D
<i>Reference catalysts</i>					
ZSM-5	30.5	ND	2–5 μm	10 MRs, 5.3 Å×5.6 Å, 5.1 Å×5.5 Å	3D
SSZ-33	32.5	ND	2–3 μm	12 MRs 6.4 Å×7.0 Å, 6.8 Å; 10 MR 5.1 Å	3D
Offretite (OFF)	3.2	ND	3–4 μm	12 MR 6.7 Å; 8 MRs 3.6 Å×4.9 Å	3D
Mordenite (MOR)	10.0	ND	1–2 μm	12 MR 6.5 Å×7.0 Å; 8 MR 2.6×5.7 Å	2D
Beta	12.0	ND	1–2 μm	12 MR 5.5 Å, 7.6 Å×6.4 Å	3D
L (LTL)	3.1	ND	Submicron	12 MR 7.1 Å	1D
USY	28.0	ND	1 μm	12 MR 7.4 Å	3D

ND: not determined.

^a As determined by elemental analysis.

^b As determined by ²⁷Al MAS NMR (octahedral aluminium is taken as non-framework).

^c As determined by SEM.

^d Si/Ga ratio.

2.2. Analytical methods

X-ray powder diffraction patterns were collected on a Scintag XDS 2000 diffractometer using Cu K_α radiation. Scanning electron micrographs (SEMs) were recorded on a Camscan Series 2-LV scanning electron microscope. Elemental analyses were performed at Galbraith Laboratories, Knoxville, TN. Solid state ²⁷Al NMR spectra were collected on a Bruker AM 300 spectrometer equipped with a cross-polarization MAS accessory. The ²⁷Al (78.2 MHz) spectra were obtained at a spinning speed of 8 KHz. The spectra were referred to 1 M aqueous aluminum nitrate solution.

2.3. Catalytic testing

The *m*-xylene reactions were carried out in a downward flow, fixed bed reactor at 317–318°C and ambient pressure. Each catalyst was first activated by heating in a flow of helium (50 ml/min STP) to 350°C. Following activation, the reactor temperature

was decreased to 317°C and the helium was directed through a saturator (*T*=10°C, *P*_{*m*-xylene}=3.4 Torr) containing *m*-xylene (99% Aldrich) absorbed on Chromosorb 102 (Supelco) before flow through the reactor. Unless otherwise stated, the carrier gas flow rate was 100 ml/min during the reaction. Inlet and outlet lines were heated to at least 120°C to prevent reactant/product condensation in the lines. In samples where a small amount of catalyst was used, an inert agent of the proper pellet size was mixed with the catalyst (quartz, Cerac, 99.5%). It was verified that addition of the quartz did not significantly affect catalyst activity or selectivity. Initial reaction rates and product distributions were obtained by extrapolating the time dependent data to zero time on stream as in [6]. The contact time (*W*_{cat}/*F*_o; *W*_{cat}=weight of catalyst, *F*_o=molar flow of *m*-xylene) was varied between 2 and 750 g cat h/mol *m*-xylene. The products were analyzed using an on-line HP 5890 Series II gas chromatograph with a 50 m HP-FFAP column and flame ionization detector. Results are reported at an *m*-xylene conversion of 10 (±2)%.

3. Results

3.1. Catalyst characterization

The XRD patterns of the unidimensional zeolites that are the main focus of this study are illustrated in Fig. 1. All the samples, with the exception of UTD-1, have XRD patterns typical of highly crystalline materials. The XRD pattern of UTD-1 has broad lines resulting from the small crystallite size of the zeolite. The porosity of the sample, which is described in [18] indicates that it is highly crystalline. The crystal size as determined by SEM, silicon/aluminum ratio, framework silicon/aluminum ratio as determined by ^{27}Al NMR and a description of the pore structure for each catalyst is contained in Table 1. The assumption is made that ratio of tetrahedral/octahedral determined by NMR is representative of the actual sample composition.

3.2. Zeolite pore system

ZSM-48 is a unidimensional zeolite bounded by 10 MRs with a diameter of $5.6 \text{ \AA} \times 5.3 \text{ \AA}$ [19]. ZSM-12 (MTW) contains a one-dimensional channel system bounded by 12 MRs [19]. The pore diameter is $5.9 \text{ \AA} \times 5.5 \text{ \AA}$. SSZ-24 is an aluminosilicate with the AFI structure. This structure possesses cylindrical pores of 7.3 \AA diameter [20,21] bounded by 12 MR. SSZ-31 (12 MR) is a highly faulted zeolite with elliptical pores in one direction. The pore diameter is 5.7 \AA in the shortest direction and 8.6 \AA in the longest direction [22]. SSZ-35 and SSZ-44 are two related high-silica zeolites. Both zeolites have a unidimensional pore system consisting of stacked cages (SSZ-44 AB stacking, SSZ-35 ABC stacking) with 10 MR pore apertures [23]. The pore diameter of SSZ-35 and SSZ-44 are 5.65 and 5.75 \AA , respectively. SSZ-42 is an aluminosilicate with an undulating, unidimensional pore system bounded by 12 MRs of 6.7 \AA diameter [24]. The undulating pore systems create cages of $11.2 \times 7.3 \times 5 \text{ \AA}$ within the zeolite [25]. MCM-58 and ITQ-4 possess the same topology as SSZ-42 (IFR). CIT-5 (CFI) contains a one-dimensional pore system bounded by constrained 14 MRs [14,26]. UTD-1 is the zeolite with the largest pores synthesized to date. The unidimensional pores system is bounded by 14 MRs, giving elliptical pores with a diameter of 7.5 \AA at the shortest point and 10.0 \AA at the longest [18,27]. Off-

retite (OFF) is a zeolite with intersecting small (8 MR) and large pores (12 MR). The 12 MR pores have a diameter of approximately 6.75 \AA [20]. Zeolite Beta (BEA) is a three-dimensional zeolite with pores bounded by 12 MRs of 5.5 and $7.6 \text{ \AA} \times 6.4 \text{ \AA}$ [20]. Zeolite L (LTL) is a low silica zeolite with a unidimensional pores system bounded by 12 MRs with a diameter of 7.1 \AA [20]. These channels open to cages of approximately 10 \AA diameter, giving LTL a stacked cage pore structure similar to SSZ-35 and SSZ-44. Mordenite, like offretite, contains intersecting channels bounded by 12 and 8 MRs. The 12 MRs create pores of $7.0 \text{ \AA} \times 6.5 \text{ \AA}$ in diameter [20]. USY is steamed, dealuminated Y (FAU) zeolite which contains both micropores and mesopores. The three-dimensional channel system contains 7.4 \AA diameter micropores bounded by 12 MRs [20]. Within the pore system the 7.4 \AA pores open into cages of approximately 13 \AA in diameter.

3.3. Reaction data

3.3.1. *p/o* Selectivity

The initial *p/o* selectivity is a useful parameter for characterizing zeolite topologies. Fig. 2 shows the initial *p/o* selectivity versus the size (or average size for non-circular pores) of the largest pore aperture for the zeolite. This type of representation, which was first introduced by Martens et al. [5], clearly shows the decreasing shape selectivity associated with larger pore zeolites.

3.3.2. *i/d* Selectivity

The ratio of the initial rates of isomerization to disproportionation also are a function of the zeolite topology. Fig. 3 illustrates the *i/d* selectivity versus the average size of the largest pore. It is evident that zeolites with large pores, those large enough to accommodate the bulky bimolecular transition state required for disproportionation, have an increased contribution of disproportionation.

3.3.3. Trimethylbenzene selectivity

The isomer distribution of trimethylbenzenes gives information concerning the pore size, shape and the presence or position of large lobes or channel intersections [5]. Larger pore zeolites tend to have a distribution of trimethylbenzenes that approaches thermodynamic equilibrium. The isomer distribution

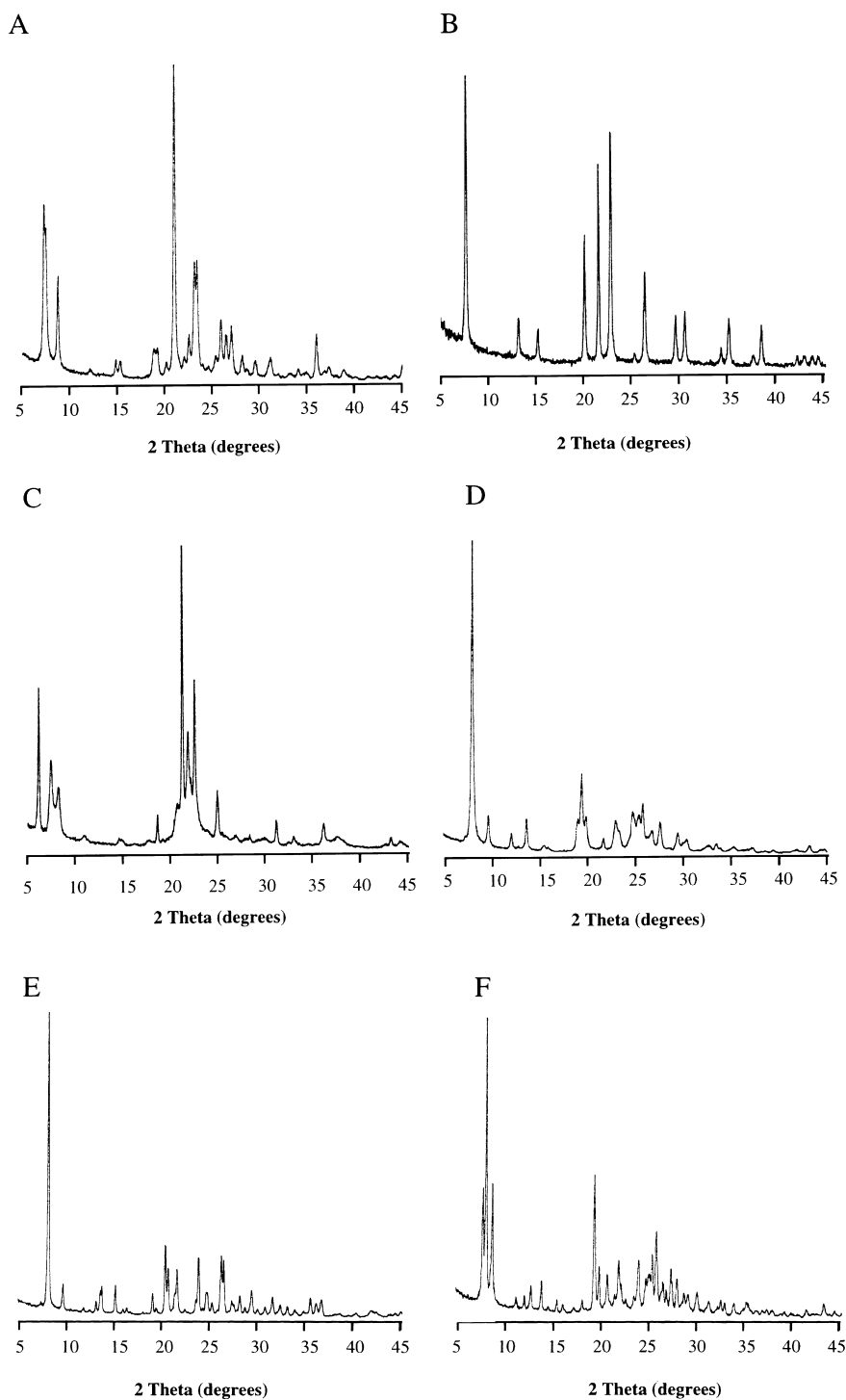


Fig. 1. XRD patterns of several molecular sieves: (a) ZSM-12; (b) SSZ-24; (c) SSZ-31; (d) SSZ-35; (e) SSZ-42; (f) SSZ-44; (g) CIT-5; (h) ZSM-48; (i) UTD-1.

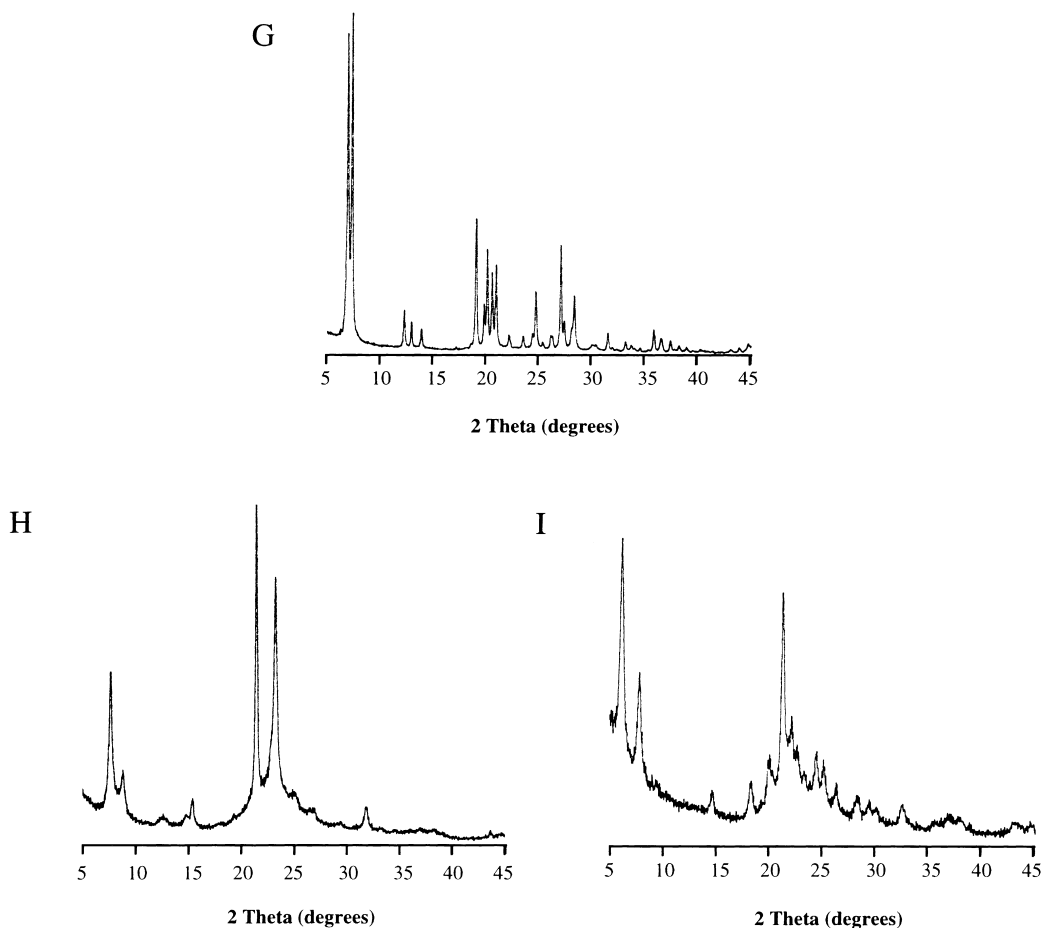


Fig. 1. (continued)

of trimethylbenzenes produced by disproportionation of *m*-xylene is enumerated in Table 2.

3.3.4. Reaction and deactivation rate

The initial rates of reaction and deactivation can be a useful indication of the pore structure of a zeolite. The activity of the zeolites studied are listed in Table 2. The deactivation rates of some of the zeolites studied are illustrated in Fig. 4.

4. Discussion

4.1. *p/o* Selectivity

The data presented in Fig. 2 show an interesting trend in the initial *p/o* selectivity for the one-dimen-

sional, large/extra-large pore catalysts such as CIT-5, SSZ-24, SSZ-31 and UTD-1. Under the conditions used in this study, all of these catalysts have a *p/o* ratio below 1 presumably due to the influence of the *ortho*-selective bimolecular isomerization mechanism. Multidimensional zeolites with roughly the same pore aperture, such as USY or Beta, have *p/o* ratios in excess of 1. It is interesting to note that LTL and USY give *p/o* ratios >1. Both these zeolites likely have enough internal porosity to accommodate the bulky bimolecular isomerization transition state due to the presence of large internal cages, yet both exhibit some *para* selectivity. Y zeolites have been studied extensively in the reaction of *m*-xylene and when the *p/o* ratio is reported, it is near 1, as is shown here [5,13,28–33]. However, it should be noted that the catalytic

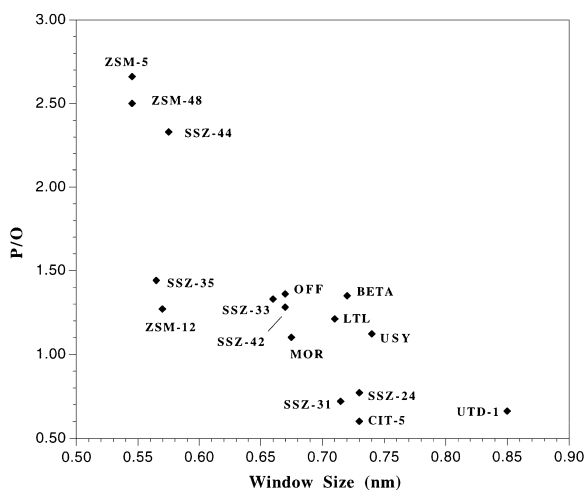


Fig. 2. Initial *p/o* selectivity in the reaction of *m*-xylene versus pore diameter of the largest pore in the zeolite. Conversion=10 (± 2)%.

performance of Y zeolites is strongly affected by parameters such as the method and degree of dealumination, alkali metal cation content, and reaction conditions [28–30]. In contrast, *p/o* selectivity is not affected to a great degree by varying parameters such as the silicon to aluminum ratio in zeolite beta [34] and this suggests that it is more reasonable for comparison

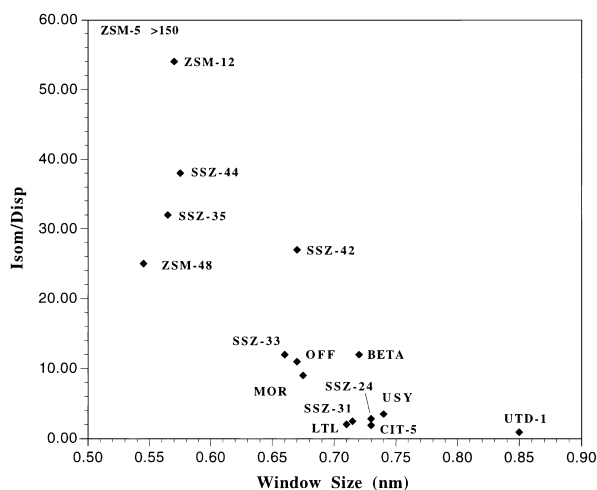


Fig. 3. Initial *i/d* selectivity in the reaction of *m*-xylene versus pore diameter of the largest pore in the zeolite. Conversion=10 (± 2)%.

to other high-silica zeolites than Y zeolites. ZSM-12 has small 12 MR pores and shows a significantly lower *p/o* ratio than would be expected from a zeolite with pores of <6.5 Å diameter [5,6]. The most striking data are the *p/o* selectivities of SSZ-35 and SSZ-44. These two zeolites are virtually identical in structure and pore size but they show distinctly different *p/o* selec-

Table 2
TMB isomer distribution and activity for reaction of *m*-xylene over different catalysts

Zeolite	1,2,3-TMB (%)	1,2,4-TMB (%)	1,3,5-TMB (%)	X_o^a (%)	Site-time yield ^b (h^{-1})
ZSM-48	NQ	100	NQ	8	0.6
ZSM-12	NQ	100	NQ	10	44.2
SSZ-24	9	83.5	7.5	10	6.8
SSZ-31	7	76	17	11	8.7
SSZ-33	8.5	72.5	19	10	19.8
SSZ-35	0	100	0	12	23.8
SSZ-42	NQ	100	NQ	11	21.9
SSZ-44	0	100	0	9	5.1
CIT-5	8	83.5	8.5	10	1.9
UTD-1	7	71	22	11	8.6
Beta	8	67	25	9	8.0
OFF	NQ	100	NQ	8	0.1
L	7	63.5	29.5	10	0.7
MORD	8.5	77.5	14	10	8.4
USY	6.5	66	27.5	10	1.2
ZSM-5	0	100	0	15	11.0
Equi. 350°C [5]	8	68	24	–	–

NQ=not quantifiable

^a Initial conversion.

^b Site defined as aluminum or gallium atom as determined by ²⁷Al MAS NMR (tetrahedral atoms) when available or elemental analysis.

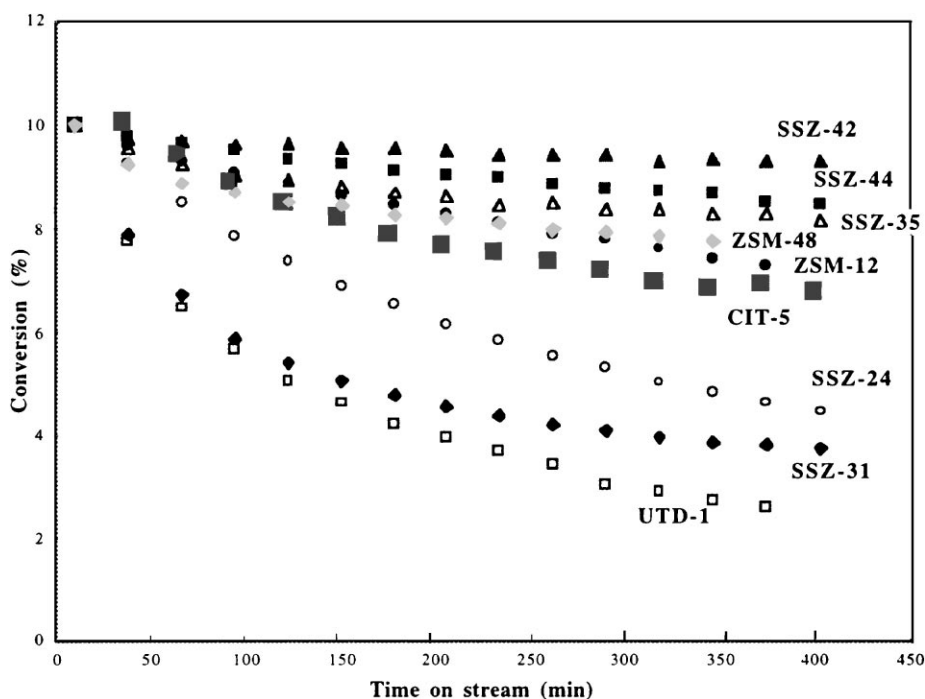


Fig. 4. Conversion versus time on stream.

tivities. In fact, SSZ-44 gives a higher p/o ratio even though it has a slightly larger pore diameter. The difference in selectivity here may be ascribed to the significantly larger crystals of SSZ-44 (Table 1), causing the zeolite to exhibit more product shape-selectivity. XRD line broadening analysis indicates that the crystals of SSZ-44 are three times larger than the SSZ-35 crystals, in agreement with SEM results. A similar effect was reported for ZSM-5, another 10 MR zeolite, by Ratnasamy et al. [35] ($8\ \mu\text{m}$: $p/o=1.2$; $12\ \mu\text{m}$: $p/o=2.25$; $16\ \mu\text{m}$: $p/o=2.55$). It is apparent that zeolites with roughly the same crystal size must be studied when comparing 10 MR zeolites. Crystal size seems less important for zeolites with 12 MRs, as reaction over mazzite (MAZ) produced virtually the same selectivity over two samples with crystal sizes differing by over an order of magnitude [5]. ZSM-5 [5,6], SSZ-33 [6], offretite [5,36], L [5,6], and mordenite [5] give p/o ratios similar to values reported in the literature for reaction under similar conditions. Results for ZSM-48 are in line with the value reported by Martens et al. [5]. Kumar and Ratnasamy [37] found ZSM-48 to be slightly more *para* selective than ZSM-5, which

is opposite to the trend found here and in the work by Martens et al. [5].

From the data in Fig. 2, it is apparent that the lowest p/o ratio for any given pore diameter appear to coincide with unidimensional zeolites having an essentially straight pore system (no cages). These lower bound zeolites include ZSM-48, ZSM-12, SSZ-31, SSZ-24, CIT-5 and UTD-1. CIT-5 contains small side pockets but it behaves similarly to the straight channel zeolites. All zeolites with multidimensional pores or with internal cages having significantly larger dimensions than the pore diameters have p/o ratios in excess of the straight channel, unidimensional zeolites.

4.2. i/d Selectivity

The largest pore zeolites have the lowest selectivity to isomerization, in agreement with previous studies of *m*-xylene reactions over zeolitic catalysts [5]. UTD-1 has the lowest i/d value of 0.9. Under the conditions used in this study, the selectivities fall into three groupings: 0–4, large pore and extra-large pore zeo-

lites, 8–14, zeolites with both 12 MR and smaller pore openings, and >20, zeolites with 10 MR openings. The three exceptions are SSZ-42, beta and ZSM-12. The peculiar internal pore architecture of SSZ-42 allows it to be quite selective for isomerization. Although it is a 12 MR zeolite, the pores of ZSM-12 are similar in size to typical 10 MR structures. In the reactions of *m*-xylene, ZSM-12 behaves like a 10 MR structure. In this work ZSM-12 is found to be slightly more selective to isomerization, than was reported previously [5]. From the data shown in Fig. 3, it appears that one-dimensional zeolites generally yield lower *i/d* ratios than multidimensional zeolites with similar pore sizes. This may be due to increased intracrystalline residence that leads to more molecular collisions and hence more bimolecular reactions. It has been reported that the *i/d* ratio cannot be used to accurately distinguish zeolites of various pore sizes [1,6]. While this is true, we show here that the *i/d* ratio does give useful information on the internal space within a zeolite. Unidimensional zeolites with large pores such as UTD-1, CIT-5, SSZ-24 and SSZ-31 all have *i/d* ratios near 1. Zeolites with internal cross-sections larger than the pore size such as USY and LTL also have *i/d* ratios near 1. These zeolites have the necessary pore space required for accommodation of the bulky bimolecular transition state. It is noteworthy that USY and LTL have significant transalkylation leading to disproportionation (*2m*-xylene → TMB + toluene) yet little transalkylation leading to isomerization (xylene1 + TMB2 → TMB1 + xylene2), which requires a slightly larger transition state. In contrast, zeolite beta has 12 MR rings but the tortuous pore system does not leave a significant amount of space that can accommodate the bimolecular transition state and *i/d* = 12. Mesoporous molecular sieves with regular pore openings behave similar to larger pore zeolites, with *i/d* near or below 1 [12,38–40].

4.3. Trimethylbenzene selectivity

The largest pore zeolite studied, UTD-1, has a TMB distribution near equilibrium. Multidimensional large pore zeolites such as USY, MOR, L and the multidimensional 12/10 MR zeolite SSZ-33 show similar selectivity. In contrast, both SSZ-24 and CIT-5, which have very similar pore openings, show a decreased production of the bulky 1,3,5-TMB. SSZ-31, which

has elliptical pore openings, has a TMB distribution more like UTD-1. For SSZ-35 and SSZ-44, the additional space created by the stacked cages apparently does not allow sufficient space to accommodate anything but the 1,2,4-isomer. At the low levels of conversion used in this work, the distribution over SSZ-42 and ZSM-12 is dominated by the 1,2,4-isomer. Both the 1,2,3- and 1,3,5- isomers are produced, but at levels too small to quantify with any precision. As expected, the smaller pore ZSM-5 catalyst shows complete selectivity to the 1,2,4-isomer. ZSM-48 produced traces of the 1,2,3- and 1,3,5-isomers but the amounts were too small to quantify. This indicates some contribution of external surface activity to overall reaction, as the micropores of this zeolite are unlikely to easily accommodate these bulky isomers. Ratnasamy and Pokhriyal [41] have reported an increase in selectivity to the 1,2,4-isomer upon surface passivation of ZSM-48.

4.4. Reaction and deactivation rate

From the data presented in Fig. 4, it is evident that the larger pore zeolites deactivate more rapidly than the smaller pore materials. SSZ-42, the undulating, unidimensional 12 MR zeolite, does not follow this trend. When the NH_4^+ form of the zeolite is loaded into the reactor prior to pretreatment, SSZ-42 does not deactivate over the first 10 h of reaction. Only a slight deactivation is observed when the NH_4^+ form is calcined and then loaded into the reactor. This slow deactivation appears to be a product of the material's unique pore structure.

Unlike the rates of deactivation, the reaction rates show no clear trend with respect to pore size. The ZSM-12 sample tested is markedly more active than expected [6]. As noted above, SSZ-44 was significantly more *para* selective than SSZ-35, which has a similar crystal structure and pore opening. This increased shape-selectivity was attributed to the significantly larger crystals of SSZ-44. The activity of these samples are in agreement with this assessment, as the site-time yield over SSZ-35 is four times that of SSZ-44, indicating the possible increased role of internal diffusional limitations caused by the large crystals of SSZ-44. The zeolites offretite and L exhibit lower site-time yields likely due to the fact that some cation sites are inaccessible to the reactants.

Table 3
Effect of flow rate on reaction activity and selectivity

Zeolite	Conversion (%)	Total flowrate (ml/min)	Contact time (h gcat/mol)	<i>p/o</i>	Site-time yield ^a (h ⁻¹)
SSZ-24	9.0	20	15.1	0.64	14.8
	9.7	99	35.3	0.77	6.8
	10.0	111	36.4	0.75	6.8
SSZ-31	11.0	54	26.8	0.80	10.6
	8.5	103	25.3	0.72	8.7
	8.8	158	24.7	0.70	9.2
UTD-1	10.0	61	12.9	0.60	18.4
	11.0	103	30.2	0.66	8.6
	12.0	143	32.4	0.65	8.8
ZSM-12	8.0	20	6.9	1.29	31.2
	10.0	102	6.1	1.27	44.2
USY	9.5	22	338.2	0.71	1.7
	10.0	103.5	514.1	1.12	1.2

^a Sites are defined as tetrahedral aluminum atoms.

4.5. Effect of external diffusion

It has been demonstrated that proper conversion/selectivity relationships must be considered when characterizing zeolites with the transformation of *m*-xylene as a test reaction [42]. Indeed, comparing zeolites at different levels of conversion leads to poor correlation between catalytic performance and zeolite structure. Most authors indicate the partial pressure of *m*-xylene, temperature and contact time when describing the reaction conditions for the *m*-xylene conversions. However, the flow rate can have a significant effect on the *p/o* selectivity. Table 3 illustrates the variation of *p/o* selectivity with flow rate at a conversion of ~9%. For zeolites with smaller pores, such as ZSM-12, the influence of flow rate is not large. However, at lower flow rates, where external diffusion can play a larger role, the *p/o* ratio is lower over larger pore catalysts. For the large pore catalysts SSZ-24, UTD-1 and USY, the *p/o* ratio increases with increasing flow rate up to a point. At sufficiently high flow rates, the *p/o* selectivity does not change significantly with flow rate. This trend implies that external diffusion effects are important at lower flow rates.

The loss in *p/o* selectivity at low flow rates is concomitant with a gain in activity per gram of catalyst. This is likely due to an increased number

of transalkylation steps involving trimethylbenzenes reacting with *m*-xylene in a bimolecular isomerization reaction. Guisnet et al. [11] reported that the most abundant TMB (1,2,4-TMB) disproportionates at a rate of an order of magnitude faster than that with which xylenes react over HY. Thus, multiple transalkylation steps are not improbable. Further support for this hypothesis is the observation that at the lower flow rates there is a corresponding decrease in the *i/d* ratio, indicating an increased amount of transalkylation. In addition, flow rate does not significantly affect the *p/o* ratio over ZSM-12, a zeolite that produces few TMBs. It is possible that the trimethylbenzenes, which were shown to be the most reactive species over HY [11], are not quickly removed from the catalyst surface due to the low carrier gas flow rate. The trimethylbenzenes can then react with *m*-xylene at or near the external surface via the bimolecular isomerization mechanism. As previously noted, Guisnet et al. [11] showed that the bimolecular isomerization is more selective for the *ortho* isomer. This increased bimolecular isomerization can explain the lower *p/o* ratios observed here at low flow rates.

A series of SSZ-33 samples were prepared to determine if the *ortho*-selective bimolecular isomerization occurs on or near (possibly in the first cage) the catalyst's external surface. The samples are described

Table 4
m-Xylene reaction over SSZ-33

Sample	Si/Al ^a	Crystal size ^b (μm)	Aluminum distribution	X_o^d	p/o_o^c	$p/o_{t=235 \text{ min}}^f$	<i>ild</i>	Total flow rate (ml/min (STP))
SSZ-33-A	32.5	2–3	Homogeneous	9.5	1.27	1.30	5.8	20
				12.5	1.35	1.34	10.0	200
SSZ-33-B	80	2–3	Homogeneous	9.5	0.98	0.91	7.0	20
				6.4	1.25	1.25	13.5	170
SSZ-33-C	53.3	2–10	Internal only	8.1	1.74	1.90	4.5	20
				8.4	1.71	1.82	7.5	100
SSZ-33-D	189.5 (17) ^c	2–10	External only	9.5	0.95	0.59	10.5	20
SSZ-33, C+D	–	–	Internal/external	8.0	1.30	0.74	5.0	20

^a As determined by elemental analysis.

^b Crystal length as determined by SEM, cigar-shaped crystals.

^c Si/B ratio.

^d Initial conversion of *m*-xylene.

^e Initial *p/o* ratio.

^f *p/o* Ratio after 235 min on stream.

in Table 4. SSZ-33-A and SSZ-33-B were prepared by exchanging aluminum for boron in the calcined zeolite via a low temperature hydrothermal treatment. This treatment results in a homogeneous distribution of aluminum in the sample [16,17]. SSZ-33-C was prepared by populating only the internal boron sites with aluminum. The as-synthesized material was first treated with trimethylsilylimidazole to cover any boron sites on the external surface. The material was then calcined and subjected to the aluminum insertion procedure used for samples A and B. SSZ-33-D was prepared such that only external sites contained aluminum, with the internal sites containing boron. The as-synthesized zeolite was subjected to the aluminum insertion procedure used for samples A–C. The SDA within the pores prevented any aluminum from replacing boron in the lattice inside the zeolite. The material was then calcined to create porosity. The borosilicate form of SSZ-33 is not active for *m*-xylene conversion under the conditions of this study.

The results for reaction over these samples are described in Table 4. For samples with a relatively low Si/Al ratio, such as SSZ-33-A, the carrier gas flow rate has only a slight effect on the reaction selectivity. In contrast, reaction over SSZ-33-B, which has a significantly higher Si/Al ratio, is markedly affected by flow rate. At low flow rates, there is a notable decrease in *p/o* selectivity, as is observed over the one-

dimensional zeolites used here. The effect of flow rate is more important for high-silica or relatively inactive samples. To obtain a given conversion a larger mass of catalyst is generally required for a high-silica zeolite (low density of acid sites) as compared to a low silica zeolite (high density of acid sites). Hence, for high-silica zeolites, a deeper bed is usually needed. This deeper bed allows for an increased probability for secondary surface mediated bimolecular isomerization. Also noteworthy is that at low flow rates, the *p/o* ratio generally declines with time on stream for catalysts with a depressed *p/o* ratio. This trend is also seen in CIT-5, SSZ-31, SSZ-24 and USY.

The *p/o* ratio resulting from reaction over SSZ-33-C showed no dependence on flow rate. The ratio is elevated compared to typical samples of SSZ-33. This increased *para* selectivity can be attributed to the loss of external surface acidic sites and to partial pore blockage during the silanation treatment. In contrast, the *p/o* ratio is very low for reaction over SSZ-33-D at low flows. In another experiment, a small portion of SSZ-33-C was dispersed in quartz chips and placed over a layer of SSZ-33-D. It was expected that *m*-xylene would react over SSZ-33-C, generating typical products. The products would then be carried down the bed and into the layer of SSZ-33-D, where the TMBs would react on the surface with *m*-xylene, giving a lower *p/o* ratio than reaction over only

SSZ-33-C. Indeed this is what results, as noted in Table 4.

These data imply that the bimolecular isomerization reaction can occur at or near the external surface. Corma et al. [13] argue that a confined pore space is needed for the bimolecular isomerization to occur and this is why it does not occur over amorphous aluminosilicates. From the data presented here, it is not clear whether the bimolecular isomerization is occurring on the external surface, within, or partially within the first cages of the zeolite. It is unlikely that sufficient space exists for significant bimolecular reaction of *m*-xylene and trimethylbenzene completely within the pores of SSZ-33. While the literature indicates that under typical reaction conditions (high flow rates) confined spaces such as micro or regular mesopores are necessary, in agreement with Corma et al., for the bimolecular isomerization to take place, this is not the case at low flow rates where external diffusional limitations are important. For a silica–alumina (35% SiO₂, pore size distribution 30–200 Å) at a flow rate 15 ml/min, a *p/o* ratio of 0.28 was obtained at a conversion of 5%.

When comparing catalysts with extremely different activities at constant conversion, either the mass of catalyst used or the carrier gas flow rate can be changed to achieve the proper conversion. It is shown here that it is paramount that the mass of catalyst be changed and the flow rate maintained the same in order to accurately compare catalysts under the same conditions in the reaction of *m*-xylene. In some cases this becomes quite difficult. Here, the mass of USY required to achieve 10% conversion of *m*-xylene was an order of magnitude larger than the mass of most other catalysts in the study. This is due to the low number of active sites and the relative weakness of these sites in the USY (CBV-760) [31]. However, if instead the flow rate is reduced to 20 from 100 ml/min, the selectivity of the catalyst changes markedly. The data in Table 3 show that at lower flow rates the catalyst produces an increased amount of *o*-xylene via the bimolecular mechanism. This decrease in *p/o* with a lower flow rate may explain the results obtained recently for reaction over USY (CBV-760) under slightly different conditions (350°C) [31]. The *p/o* ratio was found to be ~0.7, in agreement with reaction at low flow rates in this work. At higher flow rates, we found this catalyst to give *p/o* selectivity near 1, in agreement with other commercial USY zeolites in the

CBV series [31]. Additionally, carrying out the reaction at reduced flow rates for less active catalysts could explain the decrease in *p/o* ratio with a decrease in Al content for a series of MCM-41 catalysts [12].

4.6. Implications for use as a test reaction

Numerous test reactions have been proposed, but only a few have been studied in any detail. The constraint index (CI), which was originally introduced by researchers at Mobil [43], was the first quantitative method based on catalytic data for comparison of molecular sieve pore diameters. The CI is based on the competitive cracking of an equimolar mixture of *n*-hexane (HX) and 3-methylpentane (MP), with $CI = \log(\text{fraction HX unreacted}) / \log(\text{fraction MP unreacted})$. The classification developed by Mobil is as follows:

CI < 1	large pore materials
1 ≤ CI ≤ 12	medium pore materials
CI > 12	small pore materials

While there is a broad range of numerical values available for describing medium pore molecular sieves, large pore materials all fall in a narrow range of roughly 0.2–1.0. Hence, this system is not well-suited for characterizing zeolites with larger pores. In addition, MCM-22 (MWW), a zeolite with 10 MR portals and larger 12 MR cages, has a CI < 1, indicating large pore behavior. In contrast, in the reaction of *m*-xylene, MCM-22 gives a *p/o* ratio > 2, indicating 10 MR behavior [6].

Weitkamp et al. [44] proposed the spaciousness index (SI), which is based on the hydrocracking of C₁₀ naphthenes such as butylcyclohexane over a bifunctional catalyst. The SI value is the yield of isobutane/total *n*-butane. SI values for 10 MR materials all fall below 1, whereas 12 MR zeolites span a large range of 1 through > 20. Hence, this test reaction is well-suited for the characterization of the internal space in zeolites and particularly of large pore molecular sieves. However, it is not as useful for ranking medium pore materials.

It is evident that catalytic test reactions that are extremely useful for characterizing a narrow range of zeolite pore sizes exist. However, test reactions which give useful information for small, medium, large and extra-large pore molecular sieves are scarce. *m*-

Xylene conversion was expected to be of limited use for characterizing large and extra-large pore zeolites [1]. In contrast, we show here that the presence of a bimolecular pathway for isomerization allows for efficient characterization of large and extra-large pore materials. If only a monomolecular mechanism operates, the p/o ratio would be limited to values ≥ 1 . The presence of two competing mechanisms in larger pore molecular sieves gives rise to p/o ratios ranging from 0.15 for MCM-41 [12] to well above 2 for highly shape-selective small and medium pore zeolites.

Additional large and extra-large pore molecular sieves undoubtedly will be synthesized in the coming years. Meier [45] speculated that all extra-large pore structures based on four-ring building units will have one-dimensional channel structures. Indeed, both 14 MR zeolites known to date have one-dimensional channel systems (UTD-1, CIT-5). Also, several large 12 MR structures are also one-dimensional (SSZ-24, SSZ-31). In this work we show that these large and extra-large pore zeolites give p/o selectivities of less than 1. This indicates that the p/o selectivity in *m*-xylene conversion may be a simple way of identifying new unidimensional large pore materials. In fact, the low p/o selectivity for CIT-5 aided in the solution of its crystal structure.

Care should be exercised when comparing *m*-xylene reaction results from the literature. It has already been demonstrated that kinetic analysis must account for both the bimolecular and unimolecular isomerization mechanisms for zeolites where both mechanisms operate [13]. Product selectivities such as the p/o ratio are quite useful in characterizing new zeolite structures. However, we have shown here that the p/o and i/d ratios are a strong function of carrier gas flow rate for several zeolites. There is an indication that selectivity comparisons can be made between results obtained using an inert (nitrogen) or reactive (hydrogen) carrier gas [36].

5. Conclusions

The reactions of *m*-xylene are a useful tool for characterizing zeolite structures. Unlike other test reactions that are very useful but only over a narrow range of pore sizes (CI, SI), the selectivity of the reactions of *m*-xylene give information allowing one

to estimate pore diameter and architecture for medium through extra-large pore zeolites.

One-dimensional large and extra-large pore zeolites give a p/o ratio < 1 , likely due to a significant occurrence of the bimolecular isomerization mechanism. In contrast, multidimensional large pore zeolites such as USY and beta and the low-silica, unidimensional zeolite LTL give p/o ratios > 1 . The straight channel unidimensional zeolites SSZ-24, SSZ-31, CIT-5, UTD-1, ZSM-12 and ZSM-48 have the lowest p/o ratios over the range of pore sizes studied. All zeolites with multidimensional channel systems or larger cages within the micropores give higher p/o ratios. It is critical that zeolites be studied at similar levels of conversion and carrier gas flow rates in order for an accurate comparison of catalytic performance. At low flow rates the bimolecular isomerization reaction can occur to a large extent at or near the surface, leading to a lower p/o ratio.

The high-silica, unidimensional large pore zeolites (CIT-5, SSZ-24, SSZ-31, UTD-1) and zeolites with internal cages significantly larger than the pore openings (LTL, USY) give very low i/d ratios, < 2 . Large pore zeolites with sinusoidal channels (beta) and zeolites with pores $< 7 \text{ \AA}$ in diameter do not have sufficient intracrystalline space for extensive transalkylation and the i/d selectivity is > 8 .

The samples of SSZ-35 and SSZ-44, although similar in structure, give significantly different p/o ratios. This may be attributed to dissimilar crystal sizes of the two samples. SSZ-42 (IFR) behaves differently from zeolites with a similar pore size due to its unique internal structure. SSZ-42 is very selective for isomerization and it deactivates more slowly than all other zeolites studied.

Acknowledgements

CWJ thanks Akzo for financial support. Partial funding for this work provided by Chevron.

References

- [1] J. Weitkamp, S. Ernst, Catal. Today 19 (1994) 107–150.
- [2] W. Souverjins, W. Verrelst, G. Vanbutsele, J.A. Martens, P.A. Jacobs, J. Chem. Soc., Chem. Commun. (1994) 1671–1672.

- [3] A. Corma, C. Corell, F. Llopis, A. Martinez, J. Perez-Pariente, *Appl. Catal. A* 115 (1994) 121–134.
- [4] M.E. Leonowicz, J.A. Lawton, S.L. Lawton, M.K. Rubin, *Science* 264 (1994) 1910–1913.
- [5] J.A. Martens, J. Perez-Pariente, E. Sastre, A. Corma, P.A. Jacobs, *Appl. Catal. A* 45 (1988) 85–101.
- [6] B. Adair, C.Y. Chen, K.T. Wan, M.E. Davis, *Microporous Mater.* 7 (1996) 261–270.
- [7] M.A. Lanewala, A.P. Bolton, *J. Org. Chem.* 34 (1969) 3107–3112.
- [8] A. Cortes, A. Corma, *J. Catal.* 51 (1978) 338–344.
- [9] A. Corma, E. Sastre, *J. Chem. Soc., Chem. Commun.* (1991) 594–596.
- [10] A. Corma, E. Sastre, *J. Catal.* 129 (1991) 177–185.
- [11] S. Morin, N.S. Gnep, M. Guisnet, *J. Catal.* 159 (1996) 296–304.
- [12] S. Morin, P. Ayrault, S. El Mouahid, N.S. Gnep, M. Guisnet, *Appl. Catal. A* 159 (1997) 317–331.
- [13] A. Corma, F. Llopis, J.B. Monton, in: L. Guzzi et al. (Eds.), *Studies in Surface Science and Catalysis*, vol. 75, Elsevier, Amsterdam, 1993, pp. 1145–1157.
- [14] M. Yoshikawa, P.A. Wagner, M. Lovallo, K. Tsuji, T. Takewaki, C.Y. Chen, L.W. Beck, C.W. Jones, M. Tsapatsis, S.I. Zones, M.E. Davis, *J. Phys. Chem. B* 102 (1998) 7139–7147.
- [15] C.B. Dartt, M.E. Davis, *Appl. Catal. A* 143 (1996) 53–73.
- [16] S.I. Zones, US Patent, 4963 337, 1990.
- [17] C.W. Jones, S.I. Zones, M.E. Davis, *Microporous Mesoporous Mater.*, in press.
- [18] R.F. Lobo, M. Tsapatsis, C.C. Freyhardt, S. Khodabandeh, P. Wagner, C.Y. Chen, K.J. Balkus, S.I. Zones, M.E. Davis, *J. Am. Chem. Soc.* 119 (1997) 8474–8484.
- [19] J.L. Schlenker, W.J. Rohrbaugh, P. Chu, W. Valyocsik, G.T. Kokotailo, *Zeolites* 5 (1985) 355–358.
- [20] W.M. Meier, D.H. Olson, Ch. Baerlocher, *Atlas of Zeolite Structure Types*, 4th ed., Structure Commission IZA, Elsevier, London, 1996.
- [21] R. Bialek, W.M. Meier, M.E. Davis, M.J. Annen, *Zeolites* 11 (1991) 438–442.
- [22] R.F. Lobo, M. Tsapatsis, C. Freyhardt, I. Chan, C.Y. Chen, S.I. Zones, M.E. Davis, *J. Am. Chem. Soc.* 119 (1997) 3732–3744.
- [23] P.A. Wagner, S.I. Zones, R.C. Medrud, M.E. Davis, in preparation.
- [24] C.Y. Chen, W. Finger, R.C. Medrud, P.A. Crozier, I.Y. Chan, T.V. Harris, S.I. Zones, *Chem. Commun.* (1997) 1775–1776.
- [25] P.A. Barret, M.A. Camblor, A. Corma, R.H. Jones, L.A. Villaescusa, *Chem. Mater.* 9 (1997) 1713–1715.
- [26] P.A. Wagner, M. Yoshikawa, M. Lovallo, K. Tsuji, M. Tsapatsis, M.E. Davis, *Chem. Commun.* (1997) 2179–2180.
- [27] C.C. Freyhardt, M. Tsapatsis, R.F. Lobo, K.J. Balkus Jr., M.E. Davis, *Nature* 381 (1996) 295–298.
- [28] A. Corma, F. Llopis, J.B. Monton, *J. Catal.* 140 (1993) 384–394.
- [29] B. Sulikowski, *React. Kinet. Catal. Lett.* 31 (1986) 215–219.
- [30] B. Sulikowski, J. Datka, B. Gil, J. Ptaszynski, J. Klinkowski, *J. Phys. Chem. B* 101 (1997) 6929–6932.
- [31] S. Morin, P. Ayrault, N.S. Gnep, M. Guisnet, *Appl. Catal. A* 166 (1998) 281–292.
- [32] M.G. Yang, I. Nakamura, K. Fujimoto, *Appl. Catal. A* 144 (1996) 221–235.
- [33] M.G. Yang, I. Nakamura, K. Fujimoto, *Catal. Lett.* 39 (1996) 33–37.
- [34] J. Perez-Pariente, E. Sastre, V. Fornes, J.A. Martens, P.A. Jacobs, A. Corma, *Appl. Catal.* 69 (1991) 125–137.
- [35] P. Ratnasamy, G.P. Babu, A.J. Chandwadkar, S.B. Kulkarni, *Zeolites* 9 (1986) 98–100.
- [36] E. Sastre, A. Corma, F. Fajula, F. Figueras, J. Perez-Pariente, *J. Catal.* 126 (1990) 457–464.
- [37] R. Kumar, P. Ratnasamy, *J. Catal.* 118 (1989) 68–78.
- [38] X.S. Zhao, G.Q. Lu, G.J. Millar, X.S. Li, *Catal. Lett.* 38 (1996) 33–37.
- [39] T.K. Das, A.J. Chandwadkar, S. Sivasanker, *J. Mol. Catal. A* 107 (1996) 199–205.
- [40] T.K. Das, A.J. Chandwadkar, S. Sivasanker, *Microporous Mater.* 5 (1996) 401–410.
- [41] P. Ratnasamy, S.K. Pokhriyal, *Appl. Catal. A* 55 (1989) 265–269.
- [42] M. Richter, W. Fiebig, H.G. Jerschke, G. Lischke, G. Ohlmann, *Zeolites* 9 (1989) 238–246.
- [43] V.J. Frilette, W.O. Haag, R.M. Lago, *J. Catal.* 67 (1981) 218–222.
- [44] J.A. Martens, M. Tielen, P.A. Jacobs, J. Weitkamp, *Zeolites* 4 (1984) 98–107.
- [45] W.M. Meier, in: Y. Murakami et al. (Eds.), *Studies in Surface Science and Catalysis*, vol. 28, Elsevier, Amsterdam, 1986, pp. 13–22.